

## Effect of strain rate on mechanical behaviors of Ti10V2Fe3Al and 30CrMnSiNi2A<sup>①</sup>

TANG Chang-guo(唐长国)<sup>1</sup>, ZHU Jiu-hua(朱金华)<sup>2</sup>, WEI Shou-yong(魏寿庸)<sup>3</sup>

1. Department of Materials Science and Engineering,  
Donghua University, Shanghai 200051, P. R. China;

2. State Key Laboratory for Mechanical Behavior of Metallic Materials,  
Xi'an Jiaotong University, Xi'an 710048, P. R. China;

3. Northwestern Nonferrous Metals Manufacturer, Baoji 721000, P. R. China

**Abstract:** Dynamic tension tests were employed to investigate the effect of strain rate on mechanical behaviors of Ti10V2Fe3Al and 30CrMnSiNi2A. The strain rate ranges from  $10^{-4}$  to  $10^3$  s<sup>-1</sup>. Experimental results showed that the yield strength ( $\sigma_s$ ), ultimate strength( $\sigma_u$ ) and elongation( $\delta_5$ ) increase, but strain hardening exponent( $n$ ) decreases with the rise of strain rate( $\dot{\epsilon}$ ) by refractive lines. The reasons that  $\sigma_s$  and  $\sigma_u$  increase with increasing  $\dot{\epsilon}$  are concerned with thermal activation. The high strain rate induced increasing plasticity is associated with adiabatic heating of specimen, impact twinning and suppression of strain induced phase transformation. Strain hardening exponent  $n$  can be considered a constant under quasi-static loading, but decreases rapidly till an ideal plastic state( $n = 0$ ) after strain rate surpassing a critical value( $10^2$  s<sup>-1</sup>). The mechanism of  $n$  decreasing with the increase of  $\dot{\epsilon}$  is related to the increase of  $\sigma_s$  and suppression of strain induced phase transformation.

**Key words:** dynamic tension tests; strength; plasticity; strain-hardening

**Document code:** A

### 1 INTRODUCTION

Ti10V2Fe3Al and 30CrMnSiNi2A are typical materials to manufacture landing gear of airplane which bears dynamic loading during taking off and landing<sup>[1]</sup>. Aerospace spares designed by Normal Quasi-static Strength Design Criterion face the contradictory of safety and economy. Dynamic tension tests can model the practical working condition and provide believable dynamic mechanical behaviors data for design of aerospace spares. In addition, as two-phase and sub-steady materials, Ti10V2Fe3Al and 30CrMnSiNi2A have strain induced phase transformation. It has important theoretic and practical significance to study the effect of strain induced phase transformation on mechanical behaviors of materials. Ti10V2Fe3Al and 30CrMnSiNi2A with strong engineering application background were employed in the present paper to study the effect of strain rate and strain induced phase transformation on mechanical behaviors.

### 2 EXPERIMENTAL

The experimental materials were 30CrMnSiNi2A and Ti10V2Fe3Al. The heat treatment process and microstructure of tested materials were: 30CrMnSiNi2A, 1200 °C, O. Q., Martensite; Ti10V2Fe3Al, 760 °C, 2 h, W. Q. + 510 °C, 8 h, A. C.,  $\beta$ (bcc) +  $\alpha_p$ (hcp) +  $\alpha_s$ . Dynamic tension tests were conducted

using the specimens of 5 mm in diameter with a gauge length of 25 mm. The average of three measured similar data from five specimens for one strain rate test was taken as tested data. Low strain rate tension tests ( $\dot{\epsilon} = 3.3 \times 10^{-4}$ ,  $4.0 \times 10^{-3}$ ,  $3.0 \times 10^{-1}$ ,  $4.3$  s<sup>-1</sup>) were carried out on an Instron 1341 with constant extension rate, while high ones ( $\dot{\epsilon} = 2.0 \times 10^2$ ,  $8.0 \times 10^2$ ,  $1.2 \times 10^3$ ,  $1.6 \times 10^3$  s<sup>-1</sup>) on a GYC-50 rotation wheel impact test machine<sup>[2]</sup> (see Fig. 1). In impact tension tests, the impact force was measured by a strain gauge bridge which was stuck on a suffr

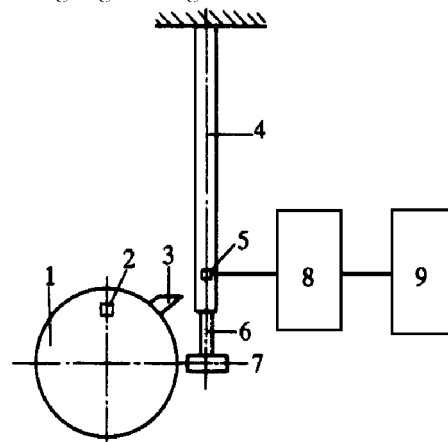


**Fig. 1** Schematic illustration of impact tension system  
1—Rotating wheel; 2—Photoelectron displacement transducer;  
3—Impact jaw; 4—Elastic output bar;  
5—Strain gauge transducer; 6—Specimen; 7—Impact block;  
8—Transient waveform storage; 9—Microcomputer

① **Foundation item:** Project 59171039 supported by the National Natural Science Foundation of China

**Received date:** Nov. 30, 1998; **accepted date:** Apr. 1, 1999

ciently long elastic output bar. In this case, the disturbance of reflection of stress wave can be avoided with this technique, a relatively smooth curve of impact force  $p$  vs time  $t$  can be obtained (see Fig. 2). The extension of specimen,  $\Delta L$ , was measured by a photoelectron displacement transducer (see Fig. 3). Thus, the strength and strain can be calculated from these curves. Because of very heavy rotating wheel and relatively thin specimen, the extension rate ( $\dot{\Delta}$ ) of specimen can be considered a constant during impact loading.

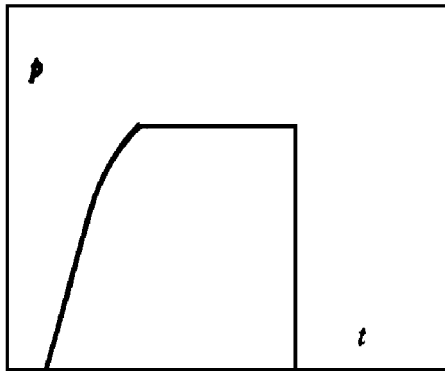


Fig. 2 Impact force  $p$  vs time  $t$

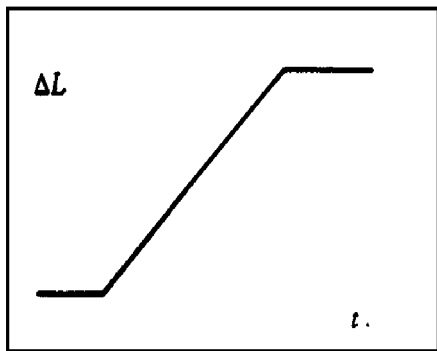


Fig. 3 Impact extension  $\Delta L$  vs time  $t$

### 3 RESULTS AND DISCUSSION

#### 3.1 High strain rate induced increasing strength and thermal activation theory

Fig. 4 shows the relation curves of  $\sigma_s$ ,  $\sigma_u$  and strain rate for tested materials. Yield strength and ultimate strength increase with increasing strain rate by refractive lines, respectively. Strengths rise slowly in the range of low strain rate, but increase rapidly in the range of high strain rate. The linear regression

expression of these refractive lines and critical strain rate  $\dot{\epsilon}_c$  of these lines are given out in Table 1.

That yield strength and ultimate strength increase with increasing strain rate by refractive lines respectively is associated with thermal activation action<sup>[3]</sup>. With the rise in strain rate, the yielding and fracturing time shorten in which the number of thermal activation atoms are used to overcome short-range energy barrier during yielding and fracturing decrease, the action of thermal activation decreases, the difficulty of crack initiation and propagation increases<sup>[4,5]</sup>, the required applied stress increases. So, the yield strength and ultimate strength increase. Through theoretic analysis and calculation, the critical strain rate of two lines approaches to the measured value<sup>[6]</sup>.

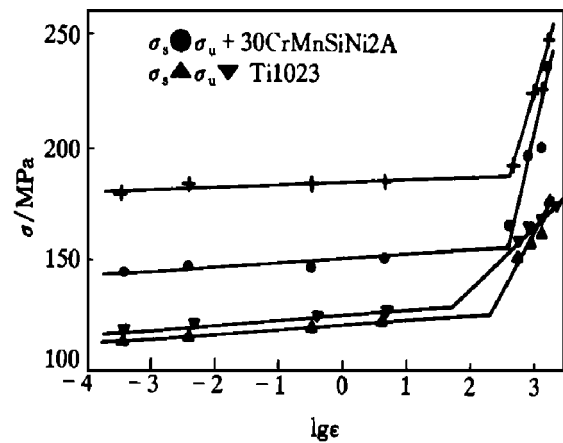


Fig. 4 Variations of  $\sigma_s$ ,  $\sigma_u$  with strain rate

#### 3.2 High strain rate induced plasticity-increasing phenomenon and mechanism

Fig. 5 shows the relation between elongation  $\delta_s$  and strain rate. It can be seen from Fig. 4 that elongation increases instead of decreasing with the rise in strain rate. Typical high strain rate induced plasticity-increasing phenomenon was found in 30CrMnSiNi2A whose elongation increases from 7% under strain rate of  $3.33 \times 10^{-4} \text{ s}^{-1}$  to 14.5% under strain rate of  $1.6 \times 10^3 \text{ s}^{-1}$ . The plasticity-increasing of 30CrMnSiNi2A and Ti10V2Fe3Al under dynamic loading improves the safety of airplane during taking off and landing.

X-ray diffraction experiment and TEM test of fractured specimens proved that the mechanism of

Table 1 Variations of  $\sigma_s$ ,  $\sigma_u$ ,  $n$  with strain rate for experimental materials

Material	$\dot{\epsilon}/\text{s}^{-1} = 3.3 \times 10^{-4} \sim 4.296$	$\dot{\epsilon}/\text{s}^{-1} = 400 \sim 1600$	$\dot{\epsilon}_c/\text{s}^{-1}$	$\dot{\epsilon}_0 (n=0)/\text{s}^{-1}$
Ti10V2Fe3Al	$\sigma_s/\text{MPa} = 1218 + 28.8 \lg \dot{\epsilon}$	$\sigma_s/\text{MPa} = 523 + 375 \lg \dot{\epsilon}$	102	
	$\sigma_u/\text{MPa} = 1240 + 26.76 \lg \dot{\epsilon}$	$\sigma_u/\text{MPa} = 836 + 282 \lg \dot{\epsilon}$	38	
	$n = 0.089 - 0.004 \lg \dot{\epsilon}$	$n = 0.62 - 0.21 \lg \dot{\epsilon}$	437	$1.03 \times 10^3$
30CrMnSiNi2A	$\sigma_s/\text{MPa} = 1498 + 21.2 \lg \dot{\epsilon}$	$\sigma_s/\text{MPa} = -1326 + 1135 \lg \dot{\epsilon}$	335	
	$\sigma_u/\text{MPa} = 1849 + 6.47 \lg \dot{\epsilon}$	$\sigma_u/\text{MPa} = -237 + 846 \lg \dot{\epsilon}$	304	
	$n = 0.34 - 0.028 \lg \dot{\epsilon}$	$n = 1.07 - 0.32 \lg \dot{\epsilon}$	324	$2.28 \times 10^3$

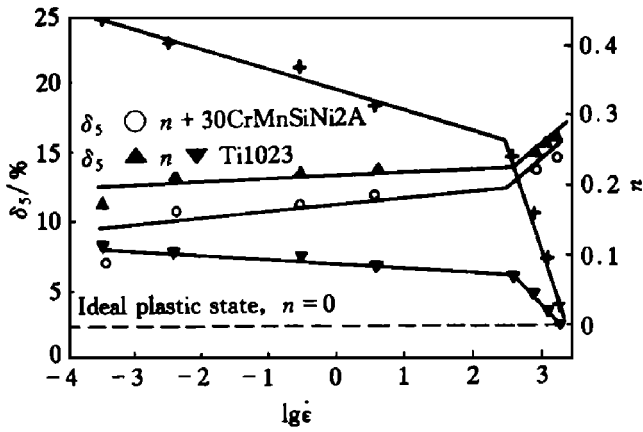


Fig. 5 Variations of  $\delta_5$  and  $n$  with strain rate

high strain rate induced plasticity increasing is associated with three factors: adiabatic heating, twinning, and suppressing of phase transformation.

Adiabatic heating is often found in materials under high strain rate loading<sup>[7]</sup>. Plastic deformation ability may be improved by adiabatic heating induced temperature rise which results in dislocation slipping easily or more slip systems beginning to slip. The temperature rising of two tested materials were found and measured in experiment<sup>[8]</sup>.

Mechanic twinning was found in 30CrMnSiNi2A at 40m/s, but not found at 8.33 $\mu$ m/s. New deformation form of twinning added to the slip mechanism contributes to the high strain rate induced plasticity increasing of 30CrMnSiNi2A<sup>[9]</sup>.

Phase transformation has happened during deformation among the tested materials. X-ray test results of Ti10V2Fe3Al are shown in Fig. 6. The diffraction peaks of undeformed specimens are two phases of  $\beta$  (110) +  $\alpha$ (001), while another peak of  $\alpha''$ (002) in 38° ~ 39° of 2 $\theta$  appears in the fractured specimen after low strain rate tension, but  $\beta$ (110) and  $\alpha$ (002) peaks instead of  $\alpha''$ (002) appear in the fractured specimens after high strain rate tension. X-ray test of the 30CrMnSiNi2A shows the microstructure of the undeformed specimen is single martensite phase but that

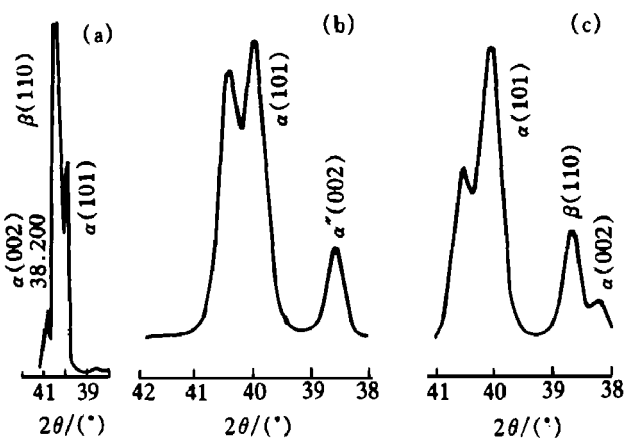


Fig. 6 X-ray diffraction results of 30CrMnSiNi2A  
(a) —Undeformed; (b) —8.33 $\mu$ m/s; (c) —40 m/s

of fractured specimen is martensite and Fe<sub>3</sub>C. The volume fraction of Fe<sub>3</sub>C or martensite changes with increasing strain rate. It is difficult to quantify the volume fractions of Fe<sub>3</sub>C and martensite(see Fig. 7). So the comparison of diffraction peak heights (minus the background) of Fe<sub>3</sub>C and martensite are calculated as follows.

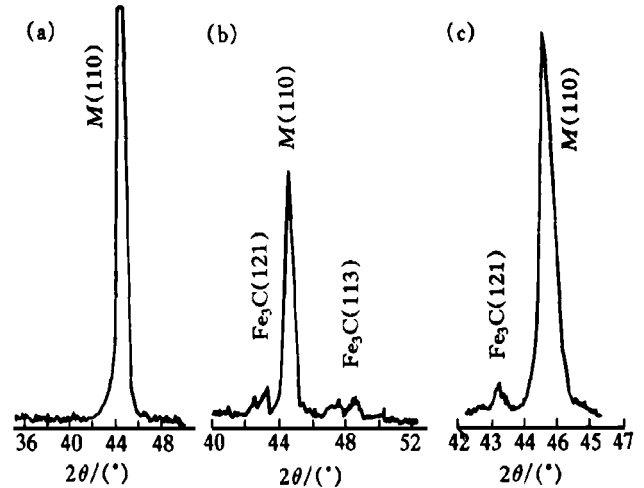


Fig. 7 X-ray diffraction results of Ti10V2Fe3Al  
(a) —Undeformed; (b) —8.33 $\mu$ m/s; (c) —40 m/s

At  $\dot{\epsilon} = 8.33 \mu\text{m/s}$ :

$$I_{\text{Fe}_3\text{C}(121)} / I_{\text{M}(110)} = 87.5 / 587.5 = 0.149$$

At  $\dot{\epsilon} = 40 \text{ m/s}$ :

$$I_{\text{Fe}_3\text{C}(121)} / I_{\text{M}(110)} = 80 / 887.5 = 0.09$$

It can be concluded from the above calculation that the Fe<sub>3</sub>C precipitated from martensite was suppressed under high velocity loading tension. The plasticity of 30CrMnSiNi2A increases by the way of suppression of hard and brittle Fe<sub>3</sub>C precipitated from martensite.

Phase transformation plays a very important role in the high strain rate induced plasticity increasing whose mechanism is different from that of TRIP steel. In addition phase transformation consumes the deformation energy and increases the deformation ability. The hard phase precipitated gradually, finely and uniformly from the soft matrix resulting in the suppression of necking, the increase of matrix strength and the keeping of deformation ability of matrix as well.

### 3.3 High strain rate induced strain hardening ability decreasing

Strain hardening exponent could be calculated from Hollomon Equation ( $\sigma = K\epsilon^n$ ), where the curve of true stress and strain transformed from that of engineering one is regressed. Fig. 4 shows that  $n$  decreases with increasing strain rate by refractive lines. Expression of  $n$  varying with strain rate, critical strain rate of turning point of refractive lines and the strain rate  $\dot{\epsilon}_0$  calculated from the linear expression of  $n$  and  $\dot{\epsilon}$  when  $n = 0$  are given in Table 1.

The following conclusions could be obtained according to Table 1.

1) If  $\dot{\epsilon} < \dot{\epsilon}_c (10^2 \sim 5 \times 10^2 \text{ s}^{-1})$ ,  $n$  decreases slowly with increasing strain rate. Therefore  $n$  can be considered a constant with an error of 2% ~ 7% for quasi-static loading.

2) If  $\dot{\epsilon} > \dot{\epsilon}_c (10^2 \sim 5 \times 10^2 \text{ s}^{-1})$ , the increase in  $\dot{\epsilon}$  will bring about a rapid decrease in  $n$  till an ideal plastic state. In this case,  $n$  can not be considered a constant. The relation between  $n$  and  $\dot{\epsilon}$  must be considered in calculation or design.

3) If  $\dot{\epsilon} = \dot{\epsilon}_0$ ,  $n = 0$ , the ideal plastic state is reached.  $\dot{\epsilon}_0 (> 10^3)$  can be estimated by extrapolation of the expression of  $n$  and  $\dot{\epsilon}$ .

In short, the deformation mode changes from strain hardening to ideal plastic state with the rise in strain rate. The mechanism that  $n$  decreases with increasing strain rate is related to the rapid increase of yield strength and suppression of strain induced phase transformation<sup>[10]</sup>. The increase in strain rate brings about a rapid increase in yield strength, which results in multi and cross slipping easily and strain hardening ability decreasing, therefore  $n$  decreasing. When strain rate approaches to a certain value, the yield strength increases so rapidly that the easy-slipping dislocation system or resource has not enough time to slip, but high stress induced dislocation resource and dislocation system begin to slip. Slipping continues to go on during deformation without increasing stress, that is the ideal plastic state. Otherwise, strain induced phase transformation will be suppressed gradually with the increase in strain rate, for examples,  $\beta$  to  $\alpha''$  phase transformation in Ti10V2Fe3Al and  $M$  to  $\text{Fe}_3\text{C}$  in 30CrMnSiNi2A. The suppression of hard and brittle  $\text{Fe}_3\text{C}$  and  $\alpha''$  precipitated from soft matrix decreases the strain hardening ability and results in  $n$  decreasing.

#### 4 CONCLUSIONS

1) With the rise in strain rate, yield strength and ultimate strength of tested materials increase slowly in low strain rate range, rapidly in high strain rate range along with refractive lines, respectively. In addition, ultimate strength grows more slowly than yield strength.

2) Elongation of tested materials rises when strain rate increases. The mechanism of high strain rate induced plasticity increasing is associated with a

diabatic heating, twinning and suppressing of strain induced phase transformation.

3) The rise in strain rate brings about strain hardening exponent decreasing by refractive lines, which is related to the increase in yield strength and the suppression of strain induced phase transformation.

4) It should be carefully considered in the design of airplane landing gear that the material's strength and elongation increase, but strain hardening exponent decreases from quasi-static loading to impact loading.

#### REFERENCES

- [1] Reinsch W A and Rosenberg H W. Three recent developments in titanium alloys [J]. Metal Progress, 1980, 20 (3): 64~ 70.
- [2] ZHANG Y H and ZHU J H. A brief introduction of GYC-50 high speed rotation wheel impact tension test machine [J]. J of Xi'an Jiaotong University, (in Chinese), 1989, 23(2): 347~ 350.
- [3] LU Bao-tong and ZHENG Xiu-lin. Thermal activation model of endurance limit [J]. Met Trans A, 1992, 23A (9): 2597~ 2605.
- [4] Xi X S and Krausz A S. Statistical theory of thermally activated fracture [J]. Journal of Mechanics, (in Chinese), 1990, 22(5): 589~ 602.
- [5] HUANG B Y, HE Y H, QU X H, *et al.* The high speed deformation induced fine grain microstructure of TiAl alloy [J]. The Chinese Journal of Nonferrous Metals, (in Chinese), 1996, 6(2): 52~ 57.
- [6] TANG C G, ZHU J H and ZHOU H J. Correlation between yield stress and strain rate for metallic materials and thermal activation approach [J]. Acta Metallurgica Sinica, (in Chinese), 1995, 31(6): A248~ 253.
- [7] YANG Y, ZHANG X M, LI Z H, *et al.* The adiabatic phenomenon in explosive welding interface of  $\alpha$ -titanium/low carbon steel [J]. The Chinese Journal of Nonferrous Metals, (in Chinese), 1995, 5(2): 93~ 97.
- [8] TANG C G, ZHU J H and ZHOU H J. A phenomenon and analysis of plasticity-increasing induced by high strain rate for some metallic materials [J]. Journal of Materials Research, (in Chinese), 1996, 10(1): 19~ 24.
- [9] YANG Y, ZHANG X M, LI Z H, *et al.* The TEM study of explosive welding interface of TA2(titanium)/A3(steel) [J]. The Chinese Journal of Nonferrous Metals, (in Chinese), 1994, 3(5): 91~ 96.
- [10] TANG C G, ZHU J H, ZHANG Y H, *et al.* Effect of strain rate on strain hardening exponent of some metallic materials [J]. Acta Metallurgica Sinica, 1996, 7(3): 183~ 186.

(Edited by PENG Chao-qun)